Eur. Phys. J. A **27**, 37–45 (2006)
DOI 10.1140/epja/i2006-10002-4

THE EUROPEAN PHYSICAL JOURNAL A

Towards a field theoretic understanding of NN → NNπ

V. Lensky[1,2], V. Baru[2], J. Haidenbauer[1], C. Hanhart[1,a], A.E. Kudryavtsev[2], and U.-G. Meißner[1,3]

[1] Institut für Kernphysik, Forschungszentrum Jülich GmbH, D-52425 Jülich, Germany
[2] Institute of Theoretical and Experimental Physics, 117259, B. Cheremushkinskaya 25, Moscow, Russia
[3] Helmholtz-Institut für Strahlen- und Kernphysik (Theorie), Universität Bonn, Nußallee 14-16, D-53115 Bonn, Germany

Received: 7 February 2006 /
Published online: 21 February 2006 –
Communicated by Th. Walcher

Abstract. We study the production amplitude for the reaction $NN \to NN\pi$ up to next-to-leading order in chiral perturbation theory using a counting scheme that takes into account the large scale introduced by the initial momentum. In particular, we investigate a subtlety that arises once the leading loop contributions are convoluted with the NN wave functions as demanded by the non-perturbative nature of the NN interaction. We show how to properly identify the irreducible contribution of loop diagrams in such type of reaction. The net effect of the inclusion of all next–to–leading-order loops is to enhance the leading rescattering amplitude by a factor of 4/3, bringing its contribution to the cross-section for $pp \to d\pi^+$ close to the experimental value.

PACS. 21.30.Fe Forces in hadronic systems and effective interactions – 12.39.Fe Chiral Lagrangians – 25.10.+s Nuclear reactions involving few-nucleon systems – 25.40.Ve Other reactions above meson production thresholds (energies > 400 MeV)

1 Introduction

The highly accurate data for pion production in nucleon-nucleon collisions close to the production threshold are a challenge for theoreticians. When the first close-to-threshold data for the total cross-section of the reaction $pp \to pp\pi^0$ appeared in 1990, existing models fell short by a factor of 5–10 [1,2]. Many different mechanisms were proposed to cure this discrepancy: heavy meson exchanges [3], (off-shell) pion rescattering [4,5], excitations of baryon resonances [6], and pion emission from exchanged mesons [7]. The total cross-sections for the reactions $pp \to pn\pi^+$ and $pp \to d\pi^+$, on the other hand, could always be described within a factor of 2 —the amplitude is dominated by the isovector rescattering contribution [1]. For a recent review, see ref. [8].

To resolve the situation various groups started to investigate $NN \to NN\pi$ using chiral perturbation theory (ChPT). As an effective field theory (EFT) it is to be free of any ambiguities and people expected that now the relevant physics of $NN \to NN\pi$ could be identified. As a big surprise to many, however, it turned out that, when naively using the original power counting by Weinberg [9], the discrepancy between theory and data became even larger at next-to-leading order (NLO) for $pp \to pp\pi^0$ [10] as well as for $pp \to d\pi^+$ [11]. At the same time it was already realized that a modified power counting is necessary to properly take care of the large momentum transfer characteristic for pion production in NN collisions, however, when applied in its original formulation the results were basically the same for neutral [12] as well as charged pions [13]. Even worse, the corrections at one-loop order (next–to–next-to-leading order ($\mathrm{N^2LO}$) in the standard counting) turned out to be even larger than the NLO corrections, indicating a divergence of the chiral expansion [14,15].

Recently, there were two developments: one that focused on some technical aspects related to the evaluation of the matrix elements [16,17] and another regarding the power counting for the large momentum transfer reactions. Formal inconsistencies of the naive power counting using the heavy baryon scheme were pointed out in ref. [18]. In addition, the ideas formulated in refs. [12,13] were further developed and improved —it was especially recognized how to properly estimate loop contributions. This scheme was implemented in refs. [19,20]— the essential features are described in detail below. The basic conclusion was that an ordering scheme exists for the reactions $NN \to NN\pi$ that can lead to a convergent series. However, so far, full calculations (including the distortions due to the NN interactions) within this scheme exist only for the production of p-wave pions [19].

[a] e-mail: c.hanhart@fz-juelich.de

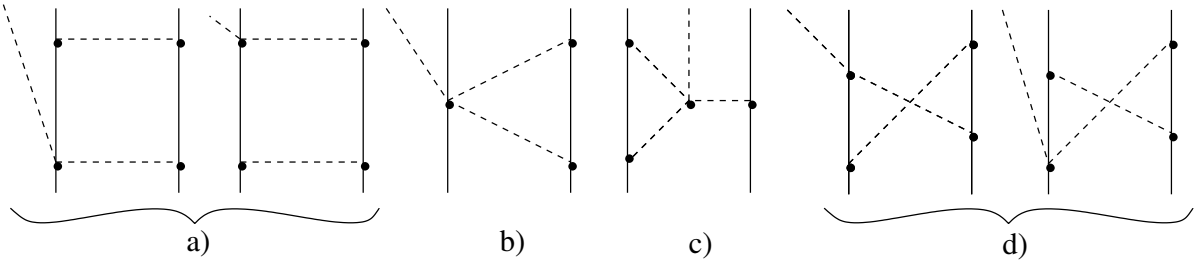

Fig. 1. Leading loop diagrams for $NN \to NN\pi$. Here dashed lines denote pions and solid lines denote nucleons.

In ref. [20] it was demonstrated by explicit evaluation of the leading loop contributions (shown in fig. 1(b)-(d)) how the presence of the large momentum scale influences loops. The central findings of that work were that it is possible to define an ordering scheme for $NN \to NN\pi$, but some loops are to be promoted to significantly lower orders compared to what is expected from Weinberg's original counting. Reference [20] left two questions unanswered that we will address in this paper:

- For the reaction channel $pp \to pp\pi^0$ the sum of all leading loops canceled; the origin of this cancellation could not be identified;
- For the channel $pp \to d\pi^+$ the sum of diagrams of fig. 1(b)-(d) gave a finite answer. However, as pointed out recently in ref. [21], the corresponding amplitudes grow linearly with increasing final NN relative momentum. This behavior leads to a large sensitivity to the final NN wave function, once the convolution of those with the transition operators is evaluated as demanded by the non-perturbative nature of the NN interaction. The solution to this problem proposed in ref. [21] is to include a new counter term at leading order to absorb this unphysical behavior. However, chiral symmetry does not allow for such a structure (see appendix for details).

As we will show in this paper, the solution to both questions is related and at the same time sheds some light on the concept of reducibility in pion reactions on few-nucleon systems.

We further demonstrate that the net effect of the inclusion of the NLO loops, shown in fig. 1, is to enhance the leading rescattering amplitude by a factor of 4/3, bringing its contribution to the cross-section for $pp \to d\pi^+$ close to the experimental value.

2 Power counting and the concept of reducibility

Already the existence of nuclei shows that perturbation theory is insufficient to properly describe two-nucleon systems: only an infinite sum of diagrams can produce a pole in the S-matrix. To bring this observation in line with power counting, Weinberg proposed to classify all possible diagrams according to the concept of reducibility [22–24]: those diagrams that have a two-nucleon cut are called reducible. Those which do not are called irreducible. The latter make up the potential that is to be constructed according to the rules of ChPT. The former are then generated by solving the Schrödinger equation, using the mentioned potential as kernel. This scheme acknowledges that the two-nucleon cut contributions are enhanced compared to the irreducible parts.

It was also Weinberg who gave a recipe how to calculate processes on few-nucleon systems with external probes [9]: here the transition operators are to be calculated using ChPT. Then those transition operators must be convoluted with the appropriate NN wave functions —in full analogy to the so-called distorted-wave Born approximation traditionally used in phenomenological calculations [1].

Therefore, it is necessary to disentangle those diagrams that are part of the wave function from those that are part of the transition operator. In complete analogy to NN scattering described above, the former are called reducible and the latter irreducible. Also here the distinction stems from whether or not the diagram shows a two-nucleon cut. Thus, in accordance to this rule, the one-loop diagrams shown in fig. 1(b)-(d) are irreducible, whereas diagrams (a) seem to be reducible. However, it will be the central finding of this work that diagrams (a) contain a genuine irreducible piece due to the energy dependence of the leading $\bar{N}N\pi\pi$ vertex, the so-called Weinberg–Tomozawa term (WT). Specifically, the energy-dependent part of the WT vertex cancels one of the intermediate nucleon propagators, resulting in the irreducible part of diagrams (a).

As mentioned in the introduction, the power counting needs to be modified in order to be applicable for $NN \to NN\pi$. The reason for this necessity is the magnitude of the nucleon center-of-mass momentum $\vec{p}$ required to produce a pion at rest in NN collisions. It is given by

$$|\vec{p}| = \sqrt{m_\pi(M + m_\pi/4)}\,, \tag{1}$$

with $M = 939\,\mathrm{MeV}$ and $m_\pi = 139.6\,\mathrm{MeV}$ denoting the nucleon and pion mass, respectively. Equation (1) exhibits the important feature of the reaction $NN \to NN\pi$, namely the large momentum mismatch between the initial and the final nucleon-nucleon state. This leads to a large invariant (squared) momentum transfer $t = -Mm_\pi$ between incoming and outgoing nucleons. The appearance of the large momentum scale $\sqrt{Mm_\pi}$ in pion production demands a change in the chiral power counting rules, as pointed out already in refs. [12,19]. In addition, it seems compulsory to include the Delta-isobar as an explicit de-

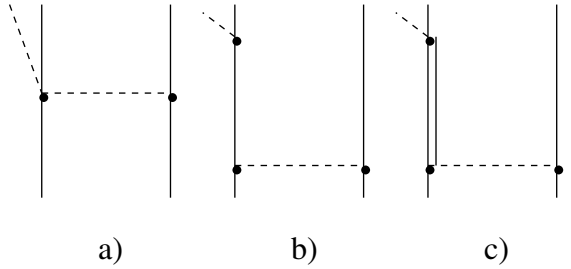

Fig. 2. Tree level diagrams that contribute at leading ((a) and (b)) and next-to-leading order (c) to $NN \to NN\pi$. The double line denotes a Δ-isobar. Note, in diagrams (b) and (c) —for illustration— with the one-pion exchange only one part of the NN and $NN \to N\Delta$ potential is shown.

gree of freedom, since the delta-nucleon mass difference $\Delta = 293\,\mathrm{MeV}$ is comparable to the external momentum $p \simeq \sqrt{M m_\pi} = 362\,\mathrm{MeV}$. The hierarchy of scales

$$m_\pi \ll p \simeq \Delta \ll M\,, \tag{2}$$

suggested by this feature, is in line with findings within meson exchange models where the Delta-isobar gives significant contributions even close to the threshold [25,26][1]. The natural expansion parameter therefore is

$$\chi = \frac{p}{M} = \sqrt{\frac{m_\pi}{M}}. \tag{3}$$

As a result at leading order only tree level diagrams contribute to the transition operator (diagrams (a) and (b) of fig. 2). Already at next-to-leading order —in addition to the first diagram that involves a Δ-isobar (diagram (c) of fig. 2)— the first loops appear (see fig. 1). As a consequence of the two scales p and m_π given in eq. (2) there exists a dimensionless parameter that is of order χ, namely m_π/p, that can appear as the argument of non-analytic functions as a result of the evaluation of loop integrals. Thus, each loop now contributes not only to a single order, but to all orders higher than the one where it starts to contribute [8]. In this work we only consider the leading parts of the loops in fig. 1 that start to contribute at NLO.

At threshold only two amplitudes are allowed to contribute to the reaction $NN \to NN\pi$, namely A_{11} and A_{10}, where we used the notation $A_{T_i T_f}$ to label the total isospin of the initial (T_i) and final (T_f) NN-pair. The third amplitude allowed by the standard selections rules —A_{01}— has to have at least one p-wave in one of the final subsystems. To the reactions $pp \to pp\pi^0$ and $pn \to pp\pi^-$ only A_{11} and to $NN \to d\pi$ only A_{10} contribute at threshold, whereas both A_{11} and A_{10} contribute to the reaction $pp \to pn\pi^+$.

The only transitions that are allowed to contribute near threshold are ${}^3P_0 \to {}^1S_0 s$ for A_{11} and ${}^3P_1 \to {}^3S_1 s$ for A_{10}, where small letters denote the pion angular momentum with respect to the NN system and the NN partial waves are labeled with the standard notation ${}^{2S+1}L_J$.

[1] For the channel $pp \to pp\pi^0$ strong support for an important role played by the Δ-isobar was given by a partial-wave analysis [27].

Those lead to the following amplitude structures [8]:

$$\mathcal{M} = iA_{11}\big((\vec{S}\cdot\vec{p})\,\mathcal{I}'\big) + A_{10}\big((\vec{S}\times\vec{p})\cdot\,\vec{S}\,'\big) \tag{4}$$

with $\mathcal{I}' = (\chi_4^\dagger \sigma_y (\chi_3^T)^\dagger)/\sqrt{2}$ and $\vec{S} = (\chi_1^T \sigma_y \vec{\sigma} \chi_2)/\sqrt{2}$ and $\vec{S}\,' = (\chi_3^\dagger \vec{\sigma} \sigma_y (\chi_4^\dagger)^T)/\sqrt{2}$, where the $\chi_{1,2}$ ($\chi_{3,4}$) denote spinors for the incoming (outgoing) nucleons. For a deuteron in the final state we need to use

$$\mathcal{M} = \tilde{A}_{10}\big((\vec{S}\times\vec{p})\cdot\,\vec{\epsilon}_d\,^*\big), \tag{5}$$

where now $\vec{\epsilon}_d\,^*$ denotes the deuteron polarization vector and $\tilde{A}_{10}$ the convolution of the production operator with the deuteron wave function —although the transition operators for A_{10} and $\tilde{A}_{10}$ are the same, the matrix elements in general have different units. We come back to the evaluation of the deuteron cross-section in sect. 4. The amplitude in eq. (4) is normalized such that for the total cross-section for $pp \to pn\pi^+$ we have

$$\sigma_{tot}(pp \to pn\pi^+) = \frac{M^3 p}{16\pi^3\sqrt{s}} \int \frac{\mathrm{d}q'\,q'^{\,2}\,p'}{\omega_{q'}} \Big(|A_{11}|^2 + 2\,|A_{10}|^2\Big), \tag{6}$$

where q' denotes the cms momentum of the outgoing π, p' the relative momentum of the outgoing pn pair, s the invariant energy of the system, and $\omega_q = \sqrt{q^2 + m_\pi^2}$. Analogously, one finds for the total cross-section for $pp \to d\pi^+$

$$\sigma_{tot}(pp \to d\pi^+) = \frac{2M_d M^2}{\pi s} q' p \big|\tilde{A}_{10}\big|^2, \tag{7}$$

where M_d denotes the deuteron mass.

If we neglect all NN distortions, we get for the leading rescattering contribution (fig. 2(a)) at threshold [20]

$$\begin{aligned} A_{11}^{2a} &= 0\,, \\ A_{10}^{2a} &= 2\left(\frac{2m_\pi}{4f_\pi^2}\right)\frac{1}{p^2 - m_\pi^2}\left(\frac{g_A}{2f_\pi}\right) \\ &= -\frac{g_A m_\pi}{2\vec{p}^{\,2} f_\pi^3}(1 + \mathcal{O}(\chi)), \end{aligned} \tag{8}$$

where we used that the $\pi N \to \pi N$ amplitude to leading order contains not only the standard WT term that scales as the sum of the incoming and outgoing pion energies, here equal to m_π and $m_\pi/2$, respectively, but also its recoil correction equal to $\vec{p}^{\,2}/2M = m_\pi/2$. The relevant terms of the underlying Lagrangian density are given in the appendix. Note that with a value of $2m_\pi/4f_\pi^2$ the WT vertex including the recoil correction as it appears in the $NN \to NN\pi$ amplitude takes exactly the value it has for elastic πN scattering at threshold.

3 Evaluation of loops

In the reaction $NN \to NN\pi$ the energies of the initial nucleons are of order $\vec{p}^{\,2}/2M \sim m_\pi$ and the momenta are of order p. In irreducible loops, on the other hand, both energies and momenta are of order p (see appendix E of

ref. [8] for details). As a consequence in the evaluation of diagrams (b),(c), and (d) of fig. 1 the nucleon recoil terms (*i.e.*, the nucleon kinetic energies) can be neglected in the nucleon propagators, since they scale as m_π. At first glance this seems to be at variance with the recent finding that three-body $NN\pi$ cuts, that originate from the nucleon recoils, play an essential role in pion reactions on few-nucleon systems [28,29]. However, the reactions studied in these references had very different kinematics, as they were small momentum transfer reactions, where in typical kinematics the πNN state was near on-shell. Here, on the other hand, we are faced with a large momentum transfer reaction: for typical kinematics a πNN intermediate state is far off-shell. In addition, here there is an additional kinematical suppression for the πNN cuts: at the cut the typical pion momentum, which set the scale for the typical loop momentum, is that of the external pion of order of at most m_π. As a consequence, the πNN cuts do not contribute before N^{5}LO to the reaction $NN \to NN\pi$ [8].

By comparison to the full results of ref. [14], in ref. [20] it was shown that it is allowed to expand the integrand of the loop integrals before evaluation in powers of $\sqrt{m_\pi/M}$. As a consequence, it was possible to express the leading contribution of all loops corresponding to diagrams (b)-(d) of fig. 1 in terms of a single integral

$$I_0(p_0,\vec{p}^{\,2}) = \frac{1}{i}\int \frac{\mathrm{d}^4 l}{(2\pi)^4}\,\frac{1}{(l_0-i\epsilon)(l^2-m_\pi^2)((l+p)^2-m_\pi^2)}\,. \tag{9}$$

One finds $I_0(p_0,\vec{p}^{\,2}) = I_0(\vec{p}^{\,2})(1+\mathcal{O}(\chi)) = 1/(16\sqrt{\vec{p}^{\,2}})(1+\mathcal{O}(\chi))$. The assumption of threshold kinematics (all outgoing momenta vanish) simplifies the operator structure significantly and we can write —neglecting for the moment the distortions from the NN interaction— in order [20]:

$$A_{10}^{1b+1c+1d} = \frac{g_A^3}{16 f_\pi^5}\,(-2+3+0)\;\vec{p}^{\,2} I_0(\vec{p}^{\,2}) = \frac{g_A^3|\vec{p}\,|}{256 f_\pi^5}\,,$$
$$A_{11}^{1b+1c+1d} = \frac{g_A^3}{16 f_\pi^5}\,(-2+3-1)\;\vec{p}^{\,2} I_0(\vec{p}^{\,2}) = 0\,. \tag{10}$$

Note, here and in what follows we write equalities although we dropped terms of higher order in χ. As mentioned in the introduction, the sum of the NLO loops vanishes in case of A_{11}. We will give an explanation for this cancellation below. Let us now concentrate on A_{10}. In order to compare the result of eq. (10) to data, the transition operators need to be convoluted with appropriate NN wave functions. The convolution integrals that arise necessarily involve non-vanishing $\vec{p}\,'$, denoting the outgoing NN relative momenta, even if we still work at threshold. However, the structure of the loop integral I_0 is such that —to leading order— only $\vec{p}-\vec{p}\,'$ appears in the integrals and thus one can directly generalize the expressions of eqs. (10). As was argued in ref. [21], this implies that for large $\vec{p}\,'$ the contributions from the loops grows linearly with $|\vec{p}\,'|$. When it then comes to the convolution of those operators with NN wave function this linear growth of the transition operators leads to a large sensitivity to the deuteron wave functions. However, there should be no sensitivity to the particular wave functions used, for off-shell quantities are not observable [30,31]. On the other hand, the chiral Lagrangian does not allow for a counter term to compensate this linear growth —see the appendix for details. The solution given in ref. [21], namely the inclusion of a counter term at leading order, is therefore not consistent with the effective field theory used. However, as we will show, the loops with the unwanted behavior will be canceled exactly by an irreducible piece of diagrams (a) of fig. 1. We proceed as follows: we first show this cancellation to one-loop order without distortions. Then, we generalize the result to the inclusion of the full NN wave functions.

We still assume threshold kinematics and now turn to the evaluation of diagrams (a) of fig. 1. In doing so one first has to realize that in contrast to the irreducible diagrams discussed in the beginning of this section, energies in the diagrams with a two-nucleon cut are of the order of the external energies ($l_0 \sim p^2/2M \sim m_\pi$). Therefore, there is *a priori* no reason to neglect the nucleon recoils that are of the order of m_π. We thus get for the full expression for the first diagram of fig. 1(a), up to higher orders,

$$A_{10}^{1a1} = i\frac{3g_A^3}{32 f_\pi^5} \times\int \frac{\mathrm{d}^4 l}{(2\pi)^4}\,\frac{\left[l_0+m_\pi-(2\vec{p}+\vec{l})\cdot\vec{l}/(2M)\right]}{\left(l_0-\frac{m_\pi}{2}-\frac{(\vec{l}+\vec{p})^2}{2M}+i\epsilon\right)\left(-l_0+\frac{m_\pi}{2}-\frac{(\vec{l}+\vec{p})^2}{2M}+i\epsilon\right)} \times\frac{(\vec{l}\cdot(\vec{l}+\vec{p}))}{(l^2-m_\pi^2)((l+p)^2-m_\pi^2)}\,,$$
$$A_{11}^{1a1} = 0\,, \tag{11}$$

where we included the recoil correction to both the WT term in the numerator as well as the nucleon energies in the denominator, in line with the discussion above. The vanishing A_{11}^{1a1} reproduces the well-known result that the WT interaction does not contribute to the leading rescattering diagram in $pp \to pp\pi^0$.

In order to proceed we rewrite the first term in the numerator of the above integral as

$$\left[l_0+m_\pi-\frac{(2\vec{p}+\vec{l})\cdot\vec{l}}{2M}\right] = \left[\left(l_0-\frac{m_\pi}{2}-\frac{(\vec{p}+\vec{l})^2}{2M}\right)+2m_\pi\right],$$

where we used that at threshold $p^2/M = m_\pi$. The first term now exactly cancels the first nucleon propagator and we are left with an expression that no longer has a two-nucleon cut —it is irreducible. In this irreducible piece we can neglect the recoil corrections in the remaining nucleon propagator —cf. the discussion at the beginning of this

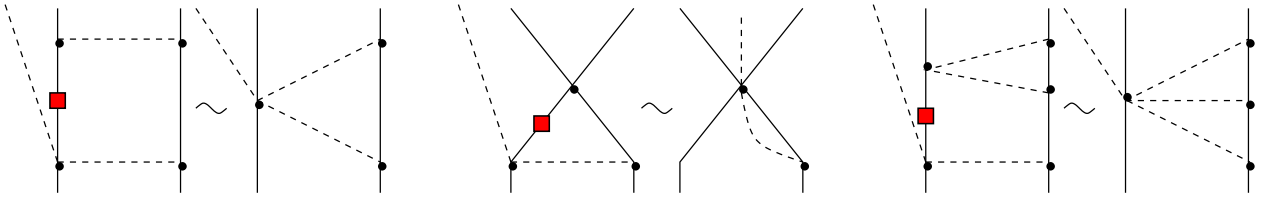

Fig. 3. Illustration of the kind of topologies that corresponds to the irreducible structures (denoted by the filled box on the propagator that gets canceled by the energy dependence of the $\pi N \to \pi N$ vertex) that emerge from the convolution of the energy-dependent rescattering term with various contributions to the NN potential.

section— and get

$$A_{10}^{1a1} = i\frac{3g_A^3}{32f_\pi^5}\int\frac{\mathrm{d}^4 l}{(2\pi)^4}\left\{\frac{(\vec{l}\cdot(\vec{l}+\vec{p}))}{(-l_0+i\epsilon)(l^2-m_\pi^2)((l+p)^2-m_\pi^2)}\right.$$
$$+\frac{2m_\pi}{\left(l_0-\frac{m_\pi}{2}-\frac{(\vec{l}+\vec{p})^2}{2M}+i\epsilon\right)\left(-l_0+\frac{m_\pi}{2}-\frac{(\vec{l}+\vec{p})^2}{2M}+i\epsilon\right)}$$
$$\left.\times\frac{(\vec{l}\cdot(\vec{l}+\vec{p}))}{(l^2-m_\pi^2)((l+p)^2-m_\pi^2)}\right\}. \qquad (12)$$

Up to higher orders the first term gives

$$A_{10}^{1a1(\mathrm{irr})} = -\left(\frac{3}{4}\right)\frac{g_A^3}{16f_\pi^5}\vec{p}^{\,2}I_0(\vec{p}^{\,2}) = -\frac{3}{4}\frac{g_A^3|\vec{p}|}{256f_\pi^5}\,, \qquad (13)$$

where the label (irr) indicates that this is only the irreducible piece of the diagram. Analogous considerations for the second diagram of diagrams (a) of fig. 1 give

$$A_{10}^{1a2} = i\frac{g_A^3}{32f_\pi^5}\int\frac{\mathrm{d}^4 l}{(2\pi)^4}\left\{\frac{(\vec{l}\cdot(\vec{l}+\vec{p}))}{(-l_0+i\epsilon)(l^2-m_\pi^2)((l+p)^2-m_\pi^2)}\right.$$
$$-\frac{2m_\pi}{\left(l_0+\frac{m_\pi}{2}-\frac{(\vec{l}+\vec{p})^2}{2M}+i\epsilon\right)\left(-l_0+\frac{m_\pi}{2}-\frac{(\vec{l}+\vec{p})^2}{2M}+i\epsilon\right)}$$
$$\left.\times\frac{(\vec{l}\cdot(\vec{l}+\vec{p}))}{(l^2-m_\pi^2)((l+p)^2-m_\pi^2)}\right\}. \qquad (14)$$

The leading piece of the first term gives

$$A_{10}^{1a2(\mathrm{irr})} = -\left(\frac{1}{4}\right)\frac{g_A^3}{16f_\pi^5}\vec{p}^{\,2}I_0(\vec{p}^{\,2}) = -\frac{1}{4}\frac{g_A^3|\vec{p}|}{256f_\pi^5}\,. \qquad (15)$$

Thus, we get

$$A_{10}^{1a1(\mathrm{irr})+1a2(\mathrm{irr})+1b+1c+1d} = \frac{g_A^3}{16f_\pi^5}\left(-\frac{3}{4}-\frac{1}{4}-2+3+0\right)\vec{p}^{\,2}I_0(\vec{p}^{\,2}) = 0\,,$$

$$A_{11}^{1a1(\mathrm{irr})+1a2(\mathrm{irr})+1b+1c+1d} = \frac{g_A^3}{16f_\pi^5}\left(0+0-2+3-1\right)\vec{p}^{\,2}I_0(\vec{p}^{\,2}) = 0\,, \qquad (16)$$

where we repeat the results for A_{11} from above for comparison. Thus, in both channels that contribute at the production threshold the sum of all irreducible loops that appear at NLO cancels[2]. On the other hand, the remaining pieces in the expressions for A_{10}^{1a} exactly agree to the convolution of the leading rescattering contribution with the one-pion exchange, however, with the $\bar{N}N\pi\pi$ WT vertex put on-shell. Thus, the WT vertex takes the value $2m_\pi/(4f_\pi^2)$ —cf. eq. (8). The two-nucleon propagators in these integrals have a unitarity cut and it is this cut contribution that should dominate the integral— in line with Weinberg's original classification as reducible and irreducible. In other words, these pieces are indeed dominated by the reducible piece[3].

Next, we show that for all ingredients of the NN potential but the one-pion exchange the choice of an on-shell $\bar{N}N\pi\pi$ vertex is of sufficient accuracy. To this end, we remind the reader that the integral corresponding to the irreducible pieces of this first diagram of fig. 1(a) had a structure like diagram (b) of that figure. This is illustrated in part (a) of fig. 3. At leading order in the NN potential there is besides the one-pion exchange also a contact interaction. The convolution of the rescattering diagram with the WT vertex (diagram (a) in fig. 2) with this part of the NN potential we can again decompose into a reducible piece with the $\pi N \to \pi N$ vertex on-shell and an irreducible piece that takes a structure of an integral with one nucleon less (see part (b) of fig. 3); this diagram, however, does not contribute below N^{4}LO and is therefore irrelevant to the order we are working. Thus, all that is to be kept is the convolution of the on-shell rescattering contribution with the contact NN interaction —in line with the findings of ref. [16]. At NLO in the NN potential there are pion loops. Then, the irreducible piece of the convolution of the leading rescattering contribution with this piece results in a two-loop diagram (for a particular example, see

[2] Using techniques similar to the extraction of the irreducible part from the 2π-exchange box graph [32], N. Kaiser has obtained the same complete cancellation for A_{11} (unpublished).

[3] In addition, the relative strength as well as sign in these terms (-3 for the pion exchange in the final $T_f = 0$ channel compared to $+1$ for the pion exchange in the initial $T_i = 1$ channel) are in agreement with the expectation values of the isospin parts of the one pion exchange in the relevant isospin channel, since $\langle TT_3|\vec{\tau}_1\cdot\vec{\tau}_2|TT_3\rangle = 2T(T+1)-3$.

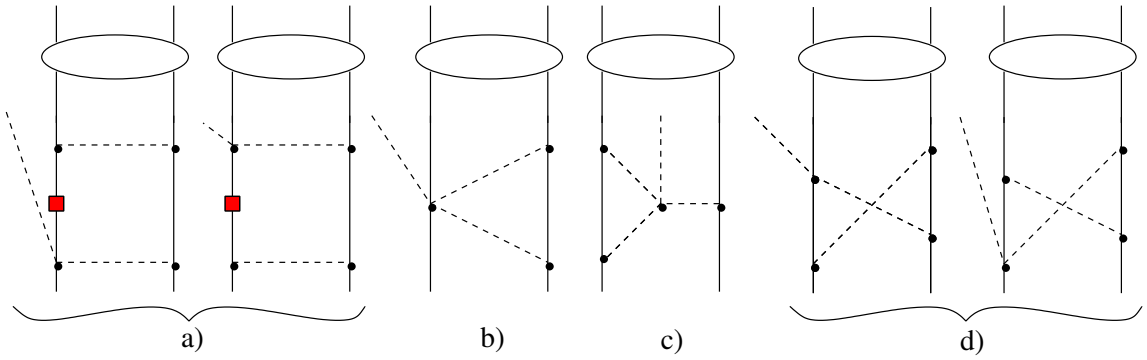

Fig. 4. Leading loop diagrams for $NN \to NN\pi$, convoluted with the NN T-matrix, denoted by the ellipse. Here dashed lines denote pions and solid lines denote nucleons. The filled box on the nucleon propagators of the diagrams (a) indicate that only the irreducible piece is to be taken. The reducible part gets absorbed into the wave function.

part (c) of fig. 3) that does not contribute up to N^{3}LO. Thus, to the order we are working we can safely put the WT vertex on-shell for the convolution of any piece of the NN potential with the leading rescattering contribution.

What remains to be shown is that the cancellation of eq. (16) survives (to the given order) the convolution with the full wave functions. This generalization is straightforward. The corresponding diagrams are shown in fig. 4 for the inclusion of the final-state interaction that we want to discuss in detail. The argument in case of the initial-state interaction is completely analogous and will not be given. Note that only the irreducible parts of the diagrams (a) are to be included —the reducible pieces get absorbed into the wave functions. Let k denote the integration variable of the convolution integral that we chose equal to the four-momentum of one of the nucleons. As argued in the previous paragraph, the integral will be dominated by energies close to the corresponding on-shell energies. This sets the scale for k —especially we can safely assume $k_0 \ll p$. This is all that is needed to neglect k_0 in the nucleon propagator of the pion loop integrals. On the other hand, in these loops $\vec{k}$ only enters as $\vec{p}-\vec{k}$. Thus, the terms that enter in the convolution integrals with the final-state interaction to the order we are working are simply given by replacing $\vec{p}$ by $\vec{p}-\vec{k}$ in eqs. (10), (13), and (15). This will obviously not change the relative strength of the individual diagrams —the cancellation survives the convolution with the wave functions. We, therefore, conclude that up to next-to-leading order all irreducible pion loops in the transition operator cancel with the only effect that the WT vertex in the rescattering diagram is to be put on-shell.

4 Results

Since the NLO diagrams discussed in this work contribute only to A_{10}, we will now discuss their impact on the reaction $pp \to d\pi^+$ that is fully determined by that amplitude. The cross-section data for this reaction near threshold is traditionally parameterized as

$$\sigma = \alpha\eta + \beta\eta^3\,, \tag{17}$$

where Coulomb effects were neglected. To the reaction $pn \to d\pi^0$ both α and β contribute with only half their strength [33]. Here, η denotes the outgoing pion momentum in units of its mass. The first term gives the s-wave strength, whereas the second one denotes the p-wave contribution (as well as some possible energy dependencies of the s-wave [21]).

Before comparison with experiment is possible, the transition operators are to be convoluted with appropriate NN wave functions. Here we use basically the same formalism as described in ref. [29][4] and thus we do not give any formulas in detail. For the NN distortions we use the CD-Bonn potential [35] and use the same parameters as in ref. [29]. To calculate the leading-order (LO) rescattering process (diagram (a) of fig. 2) we use the standard expression for the WT term in threshold kinematics —thus we put $3/2m_\pi$ at the vertex [1,36]. In addition, we also evaluate the direct contribution (diagram (b) of fig. 2). Since we derived the transition operator in threshold kinematics we can only calculate α. We obtain

$$\alpha^{LO} = 131\,\mu\text{b}. \tag{18}$$

This number is dominated by the rescattering contribution; switching off the direct term α is lowered by 30% to $\alpha^{WT,\ LO} = 101\,\mu$b. This value is consistent with those given in ref. [36]. Note that the direct term is known to be quite model dependent [36] and is small because of a cancellation of individually sizable terms. Clearly, such a cancellation cannot be captured by the counting scheme. Still, we point out that in an EFT scheme as used here all terms at a given order have to be retained.

As outlined above, in order to include the NLO contributions all we need to do is to replace the $(3/2)m_\pi$ in the WT vertex by $2m_\pi$ —or, stated differently, to scale the given results for $\alpha^{WT,\ LO}$ by a factor $(4/3)^2$. Thus, for the rescattering piece we get at NLO $\alpha^{WT,\ NLO} = 182\ \mu$b, whereas the full result including the direct term is

$$\alpha^{NLO} = 220\,\mu\text{b}. \tag{19}$$

[4] For more details, see appendix of ref. [34].

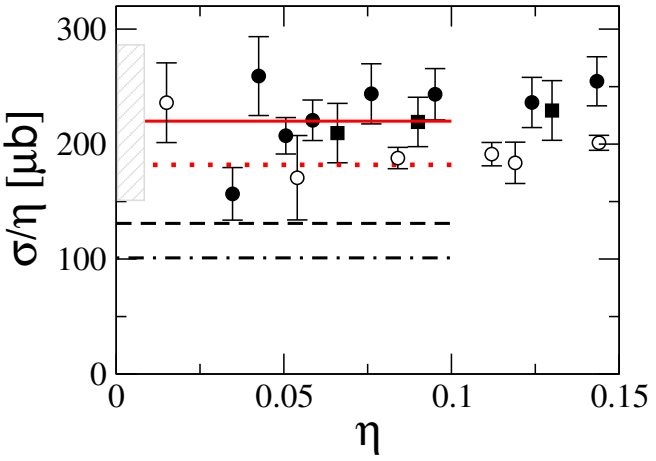

Fig. 5. Comparison of our results to experimental data for $NN \to d\pi$. The dashed and dash-dotted curves show the LO results, where for the latter the direct contribution was omitted. The solid and dotted line show the results at NLO, where in the latter the direct term was omitted. The estimated theoretical uncertainty (see text) is illustrated by the filled box. The data is from refs. [33] (open circles), [37] (filled circles) and [38] (filled squares). The first data set shows twice the cross-section for $pn \to d\pi^0$ and the other two the cross-section for $pp \to d\pi^+$.

We checked that using different models for the NN distortions changed the rescattering contribution by about 10%, in line with previous findings [36].

In fig. 5 we compare the results of our calculation to the experimental data[5]. One clearly sees that going from LO to NLO improves the description of the data. Note also that even a change by about a factor of 2 in the cross-section is in line with what is expected from the counting: after all the expansion parameter for the amplitude is $\chi = 0.4$. At the same time the relatively large expansion parameter implies a sizable theoretical uncertainty in α^{NLO} that we estimate to be of the order of $2\chi^2 \sim 30\%$ as indicated by the filled box in fig. 5. Thus, a calculation to NNLO is clearly called for.

The calculation presented is complete up to NLO from the point of view of standard chiral perturbation theory, where only nucleons and pions are treated as dynamical degrees of freedom —the effects of baryon resonances are absorbed in the counter terms. However, the ordering scheme given in eq. (2) calls in addition for an inclusion of the Delta-isobar as dynamical degree of freedom. A typical diagram is depicted in fig. 2(c) —in the calculation the full $NN \to N\Delta$ transition amplitude needs to be included. The evaluation of these diagrams needs as input the $NN \to N\Delta$ transition potential consistent with chiral symmetry. The corresponding parameters are to be fixed from a fit to NN data. Such a fit has not yet been performed and thus we postpone the evaluation of diagram (c) of fig. 2 to a later work. Note, however, that model calculations show that the contribution of the Delta-isobar is not more than 10% in the amplitude [26].

5 Summary and conclusions

We have shown that the proper set of diagrams that contributes to the transition operator for the reaction $NN \to NN\pi$ at NLO in chiral perturbation theory is given by the diagrams of fig. 2, however, with the $\bar{N}N\pi\pi$ vertex in diagram (a) put on-shell. To get to realistic results these operators are to be convoluted with proper NN wave functions. The irreducible chiral loops that arise at this order exactly cancel those terms that arise from the off-shell parts of the WT vertex. This cancellation is required for formal consistency of the whole scheme, since the mentioned diagrams show a linear growth with respect to the outgoing NN momentum. Such a growth would have led to a large sensitivity to the NN wave function, when the convolution with the final-state interaction is calculated. This, however, would have been in conflict with general arguments.

This at the same time also explains, why the sum of all loops has to vanish at next-to-leading order for the reaction $pp \to pp\pi^0$: in this channel there is no leading rescattering contribution. Thus, there is also nothing that could cancel the linear divergence discussed above. The consistency of the formalism therefore demands the sum of all loops to vanish.

As a result of our findings we can conjecture a general recipe on how to deal with pion reactions in a nuclear environment in the presence of time derivatives in vertices: one has to calculate all diagrams up to a given order, including those that are formally reducible. Then the energy dependence in the vertices is used to cancel one of the nucleon propagators. This produces an irreducible piece that is to be part of the transition operator as well as a reducible piece, where, however, the energy dependence of the vertices is replaced by the corresponding on-shell value[6].

This new rule has significant impact on the role of isoscalar rescattering in $NN \to NN\pi$ (diagram (a) of fig. 2, but with the leading isoscalar interaction used for $\pi N \to \pi N$). Empirically, the isoscalar πN scattering length is known to be very small. Theoretically, it turned out that this smallness is a consequence of an efficient cancellation amongst individually large terms [41]. Due to the energy dependence of the $\pi N \to \pi N$ operators, however, when evaluated in the kinematics relevant for pion production in NN collision this cancellation is much less efficient leading to a significant contribution from isoscalar rescattering [12,10]. If, on the other hand, the above rule is used, isoscalar rescattering enters with the strength of the very small isoscalar πN scattering length and thus would give a negligible contribution.

[5] Note that the data from $pn \to d\pi^0$ [33] are considerably lower than those for $pp \to d\pi^+$ [37,38]. It appears unclear whether this discrepancy is due to systematic uncertainties (not shown in the figure) or due to other sources [39].

[6] Note that in the presence of quadratic time derivatives at individual vertices or of the simultaneous appearance of several time derivatives in one diagram, additional vertices are to be included [40].

We have demonstrated that the net effect of the inclusion of the NLO loops, shown in fig. 1, is to enhance the leading rescattering amplitude by a factor of 4/3, bringing its contribution to the cross-section for $pp \to d\pi^+$ close to the experimental value.

The next steps will be to evaluate the $NN \to NN\pi$ amplitudes to $\mathrm{N^2LO}$ for both s- and p-wave pions for all possible amplitudes. At this order two counterterms enter for the pion s-waves and one for the pion p-waves both accompanied by S-wave nucleons in the final state. To this order p-wave pions together with P-wave nucleons are parameter-free predictions. On the other hand, there are in total more than 40 observables[7] measured for the reaction channels $pp \to pp\pi^0$ [42], $pp \to pn\pi^+$ [43], $pp \to d\pi^+$ [44] and $pn \to pp\pi^-$ [45]. Up to now only one phenomenological calculation was compared to this large amount of data [46,8] and it was found that all charged channels are well described, whereas there are significant discrepancies for the neutral pions. It will therefore be of strong interest to see if the new structures that emerge from the chiral Lagrangian are able to cure these discrepancies.

Once the described channels are analyzed within ChPT one should move ahead to consistently investigate the isospin violating observables measured recently, namely the forward-backward asymmetry in $pn \to d\pi^0$ [47] as well as the total cross-section for $dd \to \alpha\pi^0$ [48]. First steps in this direction were taken in refs. [49,50].

We thank D.R. Phillips for a stimulating discussion. We also thank the ECT* in Trento, since this work was initiated during the workshop "Charge Symmetry Breaking and Other Isospin Violations" held there in June 2005. This research is part of the EU Integrated Infrastructure Initiative Hadron Physics Project under contract number RII3-CT-2004-506078, and was supported also by the DFG-RFBR grant no. 05-02-04012 (436 RUS 113/820/0-1(R)) and the DFG-Transregionaler-Sonderforschungsbereich SFB/TR 16 "Subnuclear Structure of Matter". A.E.K, and V.B. acknowledge the support of the Federal Program of the Russian Ministry of Industry, Science, and Technology no. 40.052.1.1.1112.

Appendix A. Lagrange densities and vertices

The starting point is an appropriate Lagrangian density, constructed to be consistent with the symmetries of the underlying more fundamental theory (in this case QCD) and ordered according to a particular counting scheme. Omitting terms that do not contribute to the order we will be considering here, we therefore have for the relevant terms of the leading and next–to–leading-order Lagrangian in sigma gauge for the pion field [23]

$$\begin{aligned}
\mathcal{L} =& \frac{1}{2}\partial_\mu \boldsymbol{\pi}\partial^\mu \boldsymbol{\pi} - \frac{1}{2}m_\pi^2 \boldsymbol{\pi}^2 + \frac{1}{6f_\pi^2}\big[(\boldsymbol{\pi}\cdot\partial_\mu\boldsymbol{\pi})^2 - \boldsymbol{\pi}^2(\partial^\mu\boldsymbol{\pi}\cdot\partial_\mu\boldsymbol{\pi})\big] \\
&+ N^\dagger\left[i\partial_0 - \frac{1}{4f_\pi^2}\boldsymbol{\tau}\cdot(\boldsymbol{\pi}\times\dot{\boldsymbol{\pi}})\right]N + \frac{g_A}{2f_\pi}N^\dagger\boldsymbol{\tau}\cdot\vec{\sigma} \\
&\cdot\left(\vec{\nabla}\boldsymbol{\pi} + \frac{1}{2f_\pi^2}\boldsymbol{\pi}(\boldsymbol{\pi}\cdot\vec{\nabla}\boldsymbol{\pi})\right)N + \frac{1}{2m_N}\big[N^\dagger\vec{\nabla}^2 N + \Psi_\Delta^\dagger\vec{\nabla}^2\Psi_\Delta\big] \\
&+ \frac{1}{8M_N f_\pi^2}\big(iN^\dagger\boldsymbol{\tau}\cdot(\boldsymbol{\pi}\times\vec{\nabla}\boldsymbol{\pi})\cdot\vec{\nabla}N + \text{h.c.}\big) \\
&- \frac{g_A}{4m_N f_\pi}\big[iN^\dagger\boldsymbol{\tau}\cdot\dot{\boldsymbol{\pi}}\vec{\sigma}\cdot\vec{\nabla}N + \text{h.c.}\big] \\
&- \frac{h_A}{2m_N f_\pi}\big[iN^\dagger\boldsymbol{T}\cdot\dot{\boldsymbol{\pi}}\vec{S}\cdot\vec{\nabla}\Psi_\Delta + \text{h.c.}\big] \\
&- \frac{d_1}{f_\pi}N^\dagger(\boldsymbol{\tau}\cdot\vec{\sigma}\cdot\vec{\nabla}\boldsymbol{\pi})N\,N^\dagger N \\
&- \frac{d_2}{2f_\pi}\varepsilon_{ijk}\varepsilon_{abc}\partial_i\pi_a N^\dagger\sigma_j\tau_b N\,N^\dagger\sigma_k\tau_c N + \cdots\,, \qquad \text{(A.1)}
\end{aligned}$$

where f_π denotes the pion decay constant in the chiral limit, g_A is the axial-vector coupling of the nucleon. h_A is the $\Delta N\pi$ coupling, and $\vec{S}$ and $\boldsymbol{T}$ are the transition spin and isospin matrices, normalized such that

$$\begin{aligned}
S_i S_j^\dagger &= \frac{1}{3}\big(2\delta_{ij} - i\epsilon_{ijk}\sigma_k\big), \\
T_i T_j^\dagger &= \frac{1}{3}\big(2\delta_{ij} - i\epsilon_{ijk}\tau_k\big). \qquad \text{(A.2)}
\end{aligned}$$

The dots symbolize that what is shown are only those terms that are relevant for the calculations presented. As demanded by the heavy baryon formalism, the baryon fields N and Ψ_Δ are the velocity-projected pieces of the corresponding relativistic fields; *e.g.*, $N = 1/2(1+\not{v})\psi$, where $v^\mu = (1,0,0,0)$ denotes the nucleon 4-velocity. The corresponding vertex functions can be read off directly from appendix A of ref. [51]. The relevant vertices for the NN interaction are discussed in ref. [52].

The last two terms in eq. (A.1) show the leading four-nucleon-pion counter terms. The Pauli principle for the NN system only allows them to contribute in one fixed linear combination. The corresponding operator contributes to pion p-waves in $pp \to pn\pi^+$ as well as to the leading three-body force [19,53]. To $NN \to NN\pi$ at threshold this operator can only contribute through loops. The leading four-N-π vertices that contribute there are suppressed by an additional m_π/M [12,10]. In general, to be in line with the Goldstone theorem, it is a necessary requirement that counter terms either contain a derivative acting on the pions, or scale with m_π^2. The latter is a consequence of the well-known relation $m_\pi^2 \propto \hat{m}$, where $\hat{m}$ denotes the average mass of the light quarks. To be consistent with chiral symmetry the chiral Lagrangian is only allowed to have terms analytic in $\hat{m}$. To absorb the sensitivity to the wave function discussed in the introduction would require a counter term that neither contains powers of m_π nor a derivative acting on the pion field at variance with chiral symmetry.

[7] This large number is achieved by fully exploiting the 5-dimensional phase space [42].

References

1. D. Koltun, A. Reitan, Phys. Rev. **141**, 1413 (1966).
2. G.A. Miller, P. Sauer, Phys. Rev. C **44**, 1725 (1991).
3. T.-S.H. Lee, D. Riska, Phys. Rev. Lett. **70**, 2237 (1993); C.J. Horowitz, H.O. Meyer, D.K. Griegel, Phys. Rev. C **49**, 1337 (1994) (arXiv:nucl-th/9304004).
4. E. Hernández, E. Oset, Phys. Lett. B **350**, 158 (1995) (arXiv:nucl-th/9503019).
5. C. Hanhart *et al.*, Phys. Lett. B **358**, 21 (1995) (arXiv:nucl-th/9508005).
6. M.T. Peña, D.O. Riska, A. Stadler, Phys. Rev. C **60**, 045201 (1999) (arXiv:nucl-th/9902066).
7. U. van Kolck, G.A. Miller, D.O. Riska, Phys. Lett. B **388**, 679 (1996) (arXiv:nucl-th/9607026).
8. C. Hanhart, Phys. Rep. **397**, 155 (2004) (arXiv:hep-ph/0311341).
9. S. Weinberg, Phys. Lett. B **295**, 114 (1992).
10. B.Y. Park *et al.*, Phys. Rev. C **53**, 1519 (1996) (arXiv:nucl-th/9512023).
11. C. Hanhart, J. Haidenbauer, M. Hoffmann, U.-G. Meißner, J. Speth, Phys. Lett. B **424**, 8 (1998) (arXiv:nucl-th/9707029).
12. T.D. Cohen, J.L. Friar, G.A. Miller, U. van Kolck, Phys. Rev. C **53**, 2661 (1996) (arXiv:nucl-th/9512036).
13. C. da Rocha, G. Miller, U. van Kolck, Phys. Rev. C **61**, 034613 (2000) (arXiv:nucl-th/9904031).
14. V. Dmitrašinović, K. Kubodera, F. Myhrer, T. Sato, Phys. Lett. B **465**, 43 (1999) (arXiv:nucl-th/9902048).
15. S.I. Ando, T.S. Park, D.P. Min, Phys. Lett. B **509**, 253 (2001) (arXiv:nucl-th/0003004).
16. C. Hanhart, G.A. Miller, F. Myhrer, T. Sato, U. van Kolck, Phys. Rev. C **63**, 044002 (2001) (arXiv:nucl-th/0010079).
17. A. Motzke, C. Elster, C. Hanhart, Phys. Rev. C **66**, 054002 (2002) (arXiv:nucl-th/0207047); V. Malafaia, M.T. Peña, Phys. Rev. C **69**, 024001 (2004) (arXiv:nucl-th/0312017); Y. Kim, I. Danchev, K. Kubodera, F. Myhrer, T. Sato, arXiv:nucl-th/0509004.
18. V. Bernard, N. Kaiser, U.-G. Meißner, Eur. Phys. J. A **4**, 259 (1999) (arXiv:nucl-th/9806013).
19. C. Hanhart, U. van Kolck, G. Miller, Phys. Rev. Lett. **85**, 2905 (2000) (arXiv:nucl-th/0004033).
20. C. Hanhart, N. Kaiser, Phys. Rev. C **66**, 054005 (2002) (arXiv:nucl-th/0208050).
21. A. Gårdestig, talk presented at the *ECT* workshop Charge Symmetry Breaking, Other Isospin Violations, Trento, June 2005*; A. Gårdestig, D.R. Phillips, C. Elster, arXiv:nucl-th/0511042.
22. S. Weinberg, Phys. Lett. B **251**, 288 (1990); Nucl. Phys. B **363**, 3 (1991).
23. C. Ordóñez, L. Ray, U. van Kolck, Phys. Rev. Lett. **72**, 1982 (1994); Phys. Rev. C **53**, 2086 (1996).
24. E. Epelbaum, W. Glöckle, U.-G. Meißner, Nucl. Phys. A **637**, 107 (1998) (arXiv:nucl-th/9801064).
25. J.A. Niskanen, Phys. Rev. C **53**, 526 (1996) (arXiv:nucl-th/9502015).
26. C. Hanhart, J. Haidenbauer, O. Krehl, J. Speth, Phys. Lett. B **444**, 25 (1998) (arXiv:nucl-th/9808020).
27. P.N. Deepak, J. Haidenbauer, C. Hanhart, Phys. Rev. C **72**, 024004 (2005) (arXiv:hep-ph/0503228).
28. V. Baru, C. Hanhart, A.E. Kudryavtsev, U.-G. Meißner, Phys. Lett. B **589**, 118 (2004) (arXiv:nucl-th/0402027).
29. V. Lensky, V. Baru, J. Haidenbauer, C. Hanhart, A.E. Kudryavtsev, U.-G. Meißner, Eur. Phys. J. A **26**, 107 (2005) (arXiv:nucl-th/0505039).
30. R. Haag, Phys. Rev. **112**, 669 (1958).
31. H. Lehmann, K. Symanzik, W. Zimmermann, Nuovo Cimento **1**, 205 (1955).
32. N. Kaiser, Phys. Rev. C **62**, 024001 (2000) (arXiv:nucl-th/9912054).
33. D.A. Hutcheon *et al.*, Nucl. Phys. A **535**, 618 (1991).
34. V.E. Tarasov, V.V. Baru, A.E. Kudryavtsev, Phys. At. Nucl. **63**, 801 (2000).
35. R. Machleidt, Phys. Rev. C **63**, 024001 (2001) (arXiv:nucl-th/0407003).
36. C.J. Horowitz, Phys. Rev. C **48**, 2920 (1993).
37. P. Heimberg *et al.*, Phys. Rev. Lett. **77**, 1012 (1996).
38. M. Drochner *et al.*, Nucl. Phys. A **643**, 55 (1998).
39. H. Machner, J. Niskanen, arXiv:nucl-ex/0511027.
40. I.S. Gerstein, R. Jackiw, B.W. Lee, S. Weinberg, Phys. Rev. D **3**, 2486 (1971).
41. V. Bernard, N. Kaiser, U.-G. Meißner, Phys. Lett. B **309**, 421 (1993) (arXiv:hep-ph/9304275).
42. H.O. Meyer *et al.*, Phys. Rev. C **65**, 027601 (2001).
43. W.W. Daehnick *et al.*, Phys. Rev. C **65**, 024003 (2002) (arXiv:nucl-ex/0108021).
44. B. von Przewoski *et al.*, Phys. Rev. C **61**, 064604 (2000) (arXiv:nucl-ex/9912008).
45. M. Daum *et al.*, Eur. Phys. J. C **23**, 43 (2002) (arXiv:nucl-ex/0108008); **25**, 55 (2002) (arXiv:nucl-ex/0112011).
46. C. Hanhart, J. Haidenbauer, O. Krehl, J. Speth, Phys. Rev. C **61**, 064008 (2000) (arXiv:nucl-th/0002025).
47. A.K. Opper *et al.*, Phys. Rev. Lett. **91**, 212302 (2003) (arXiv:nucl-ex/0306027).
48. E.J. Stephenson *et al.*, Phys. Rev. Lett. **91**, 142302 (2003) (arXiv:nucl-ex/0305032).
49. U. van Kolck, J.A. Niskanen, G.A. Miller, Phys. Lett. B **493**, 65 (2000) (arXiv:nucl-th/0006042).
50. A. Gårdestig *et al.*, Phys. Rev. C **69**, 044606 (2004) (arXiv:nucl-th/0402021).
51. V. Bernard, N. Kaiser, U.-G. Meißner, Int. J. Mod. Phys. E **4**, 193 (1995) (arXiv:hep-ph/9501384).
52. E. Epelbaum, to be published in Prog. Nucl. Part. Phys., arXiv:nucl-th/0509032.
53. E. Epelbaum, A. Nogga, W. Glöckle, H. Kamada, U.-G. Meißner, H. Witala, Phys. Rev. C **66**, 064001 (2002) (arXiv:nucl-th/0208023).